

## LIFETIME STUDIES AT THE APS

**Annick Ropert, ESRF**

### Plan

The studies presented in this note are focused on the lifetime characterization with positrons for the symmetrical low  $\beta_y$  lattice. Before switching back to electrons, detailed lifetime studies were performed in order to gather data that could be compared to similar ones with electrons, the ultimate goal being to define a model that could be used to predict lifetimes. The report is divided into three parts:

- simulations to allow decoupling of the different contributions to the lifetime
- review of the experimental conditions and related problems
- analysis of the data and discussion of the limitations

### Experimental data

Typical data gathered during operation with a standard filling pattern (fill at 100 mA with 10 mA in 6 buckets plus 90 mA in 25 triplets) are plotted in Figures 1 to 3. They clearly show that the lifetime (of the order of 29 h at 100 mA) is Touschek dominated.

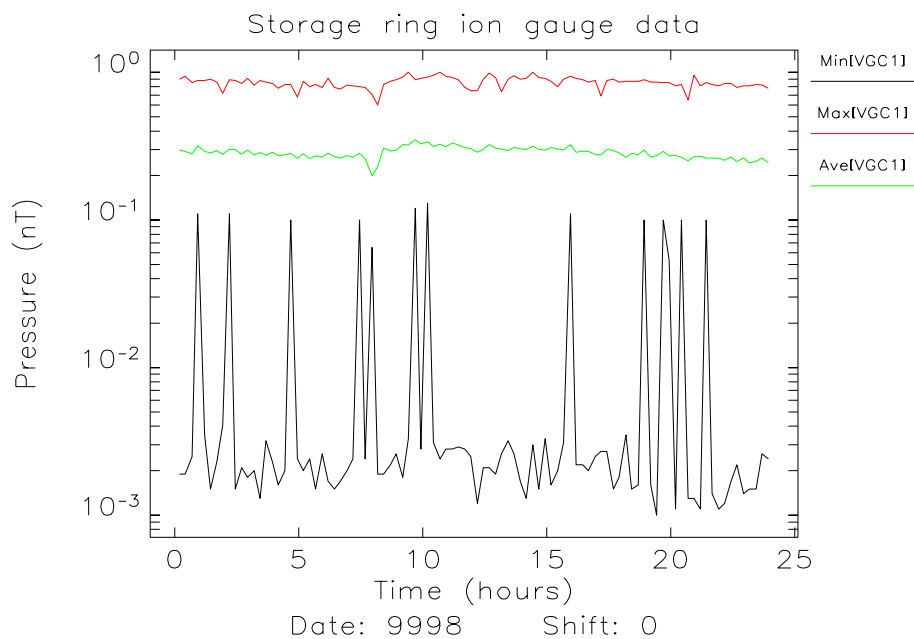


**Figure 1:** Average pressure from the ion gauges over a 24 h period

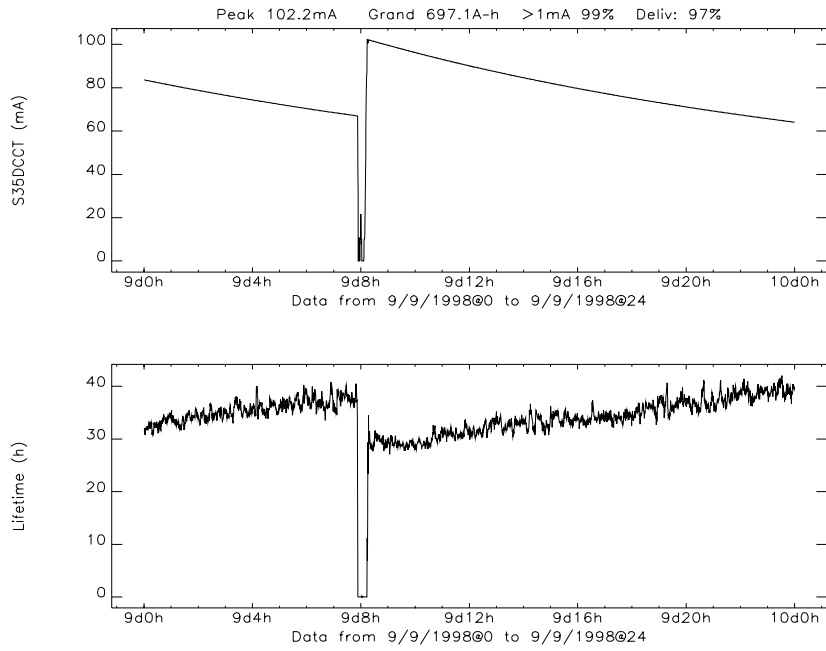


**Figure 2:** Intensity and lifetime over a 24 h period

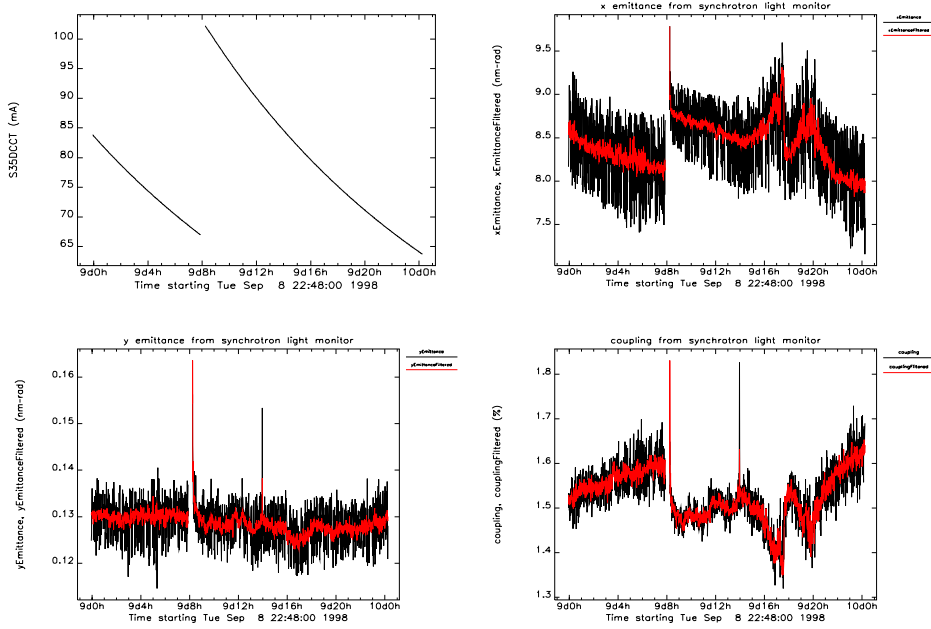


**Figure 3:** Intensity, horizontal emittance, vertical emittance, coupling over a 24 h period

Some estimations of the contributions to the lifetime at 100 mA from elastic gas scattering, Bremsstrahlung, and Touschek are given in Table 1. These estimations are used with the data in Table 2 for low  $\beta_y$  optics.

Table 1

elastic scattering	Bremsstrahlung	Touschek	total
270 h	251 h	39 h	30 h

Table 2

average pressure	0.5	nT
gas composition	H <sub>2</sub> : 48 H <sub>2</sub> O: 24 N <sub>2</sub> : 12 H <sub>2</sub> : 12 CO <sub>2</sub> : 4	%
average $\beta_y$	15.76	m
transverse acceptance	$9.25 \cdot 10^{-7}$	m.rad
horizontal emittance	$8.6 \cdot 10^{-9}$	m.rad
coupling	1.6	%
I / bunch	1.2	mA
$V_{RF}$	9.5	MV
bunch lengthening	1.6	
bunch length	8.5	mm
energy acceptance	1.7	%

### **Definition of adequate measuring conditions for each contribution**

It is evident from Table 2 that precise modeling of the lifetime depends on many parameters (transverse and longitudinal beam sizes, rf voltage, synchrotron and parasitic beam losses, energy acceptance, aperture limitations, average pressure and residual gas composition,...).

Since the objective is to determine more precisely the different rates, and since the small transverse emittances make the machine Touschek dominated, dedicated experimental conditions have to be defined in order to decouple the different contributions to the lifetime and minimize the influence of uncertainties on the measured parameters contributing to the lifetime computations.

### ⊗ Vertical elastic gas scattering:

The elastic gas scattering lifetime depends on the transverse acceptance  $A$  and on the gas composition (defined by the residual pressure  $p_i$ , the atomic number  $Z_j$ , and the number of atoms per molecule  $\alpha_{ij}$  of the different species) in the following way:

$$\frac{1}{\tau_G} = C_G \frac{\beta_A}{A^2} \sum_{atomj} \left[ Z_j^2 \sum_{gasi} \alpha_{ij} \langle \beta_{x,y} p_i \rangle \right],$$

where  $C_G$  is a constant and  $\beta_A$  is the  $\beta$  function at the location where the transverse acceptance is limited.

Imposing an additional aperture reduction with respect to the present  $\pm 2.5$  mm vertical physical aperture of the ID3 straight section by progressively closing the vertical jaws of the sector 38 scraper (located downstream the B:QD4 quadrupole at a  $\beta_y$  of 31.63 m) and recording the resulting lifetime evolution should, in principle, enable the pressure contribution to be fully determined.

The minimization of the Touschek contribution for this experiment requires a small current per bunch. This can be obtained by filling the machine at 100 mA with a uniform filling pattern (for instance with a  $83 * 10$  filling pattern, the Touschek lifetime is increased by more than a factor of 6, when taking into account the reduction of lifetime that results from the quasi absence of bunch lengthening for a 0.12 mA / bunch).

An additional factor can be obtained by running the machine with a large coupling that can be controlled by moving the tunes closer to the coupling resonance. In this case, the achievable maximum coupling is guided by APS previous experience with trips triggered by the ID3 radiation monitors. Although the vertical beam size at the end of the straight section (only of the order of 100  $\mu\text{m}$  with a 10% coupling, as compared to the  $25\sigma$  given by the 2.5 mm high vacuum vessel) should not induce any trip, a 5% coupling is contemplated.

Simulations have been performed with these conditions. They are summarized in Figure 4 and indicate that the zone of interest is between 0.65 mm (quantum limit) and 2.5 mm (above this scraper aperture, the contribution of the other lifetimes starts to be too large).

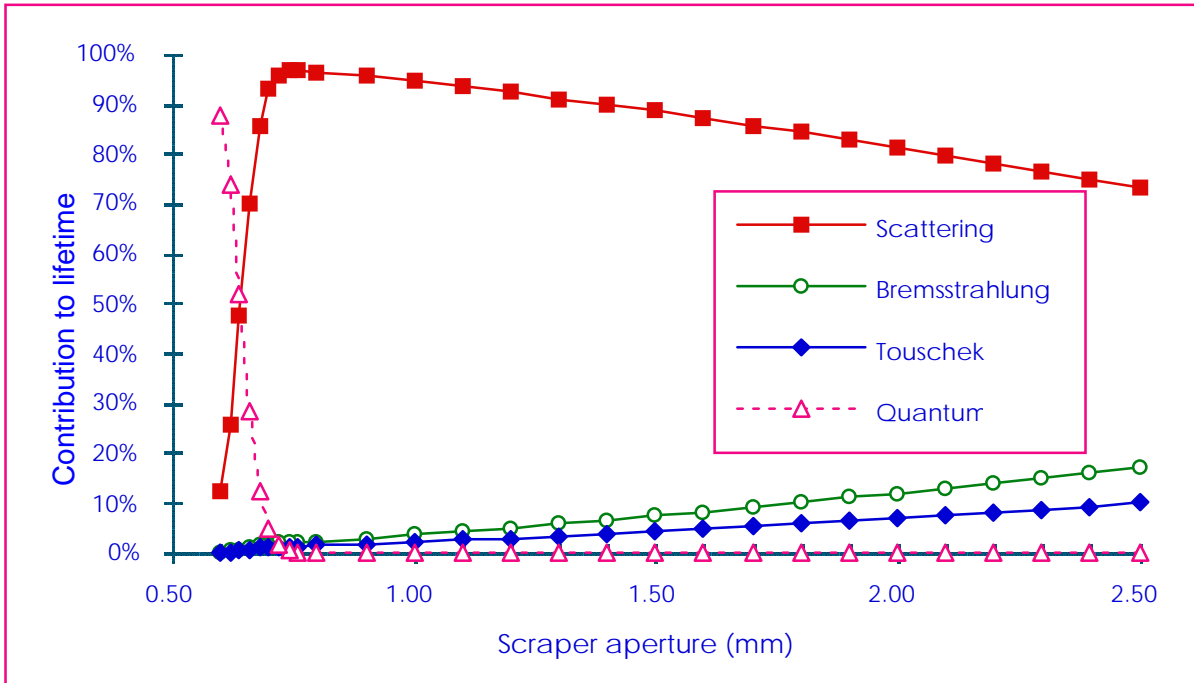


**Figure 4:** Evolution of the different contributions to the lifetime when scraping the beam

To obtain a better estimate of the gas rate, the experiment can be reproduced at different intensities; as shown in Figure 5, the weight of the different lifetimes hardly changes.

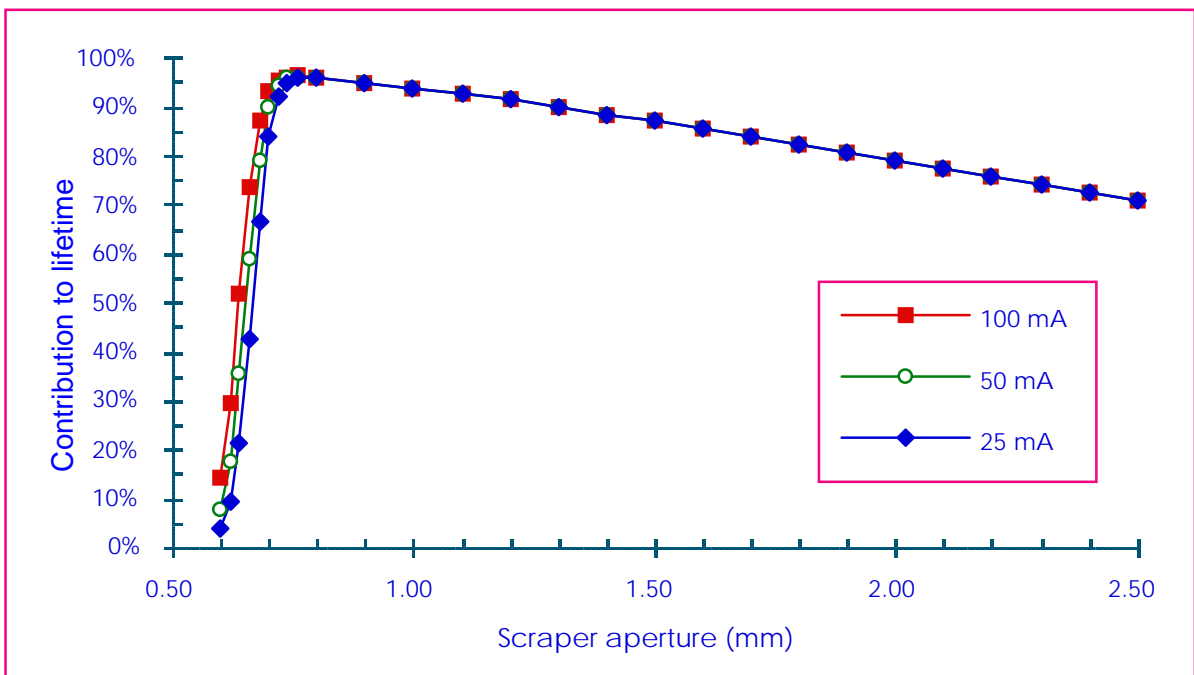


**Figure 5:** Influence of the intensity on the different lifetime contributions when scraping the beam

### ☞ Bremsstrahlung:

The inelastic gas scattering (or Bremsstrahlung) component is given by the formula:

$$\frac{1}{\tau_B} = C_B \left[ -\frac{4}{3} \ln \frac{\Delta p}{p} - \frac{5}{6} \right] \sum_{\text{atomj}} \left[ Z_j^2 \ln \frac{183}{Z_j^{1/3}} \sum_{\text{gasi}} \alpha_{ij} p_i \right],$$

where  $C_B$  is a constant and  $\Delta p/p$  is the energy acceptance. The pressure coefficients are the same as for the elastic gas scattering.

Modeling of the Bremsstrahlung contribution is more delicate since it is never the dominant contribution to the lifetime. The method consists of recording the evolution of the lifetime versus the rf voltage in conditions where the Touschek contribution is minimized. The pressure dependence of the Bremsstrahlung lifetime is supposed to be known from the gas scattering experiment.

Results of simulations are shown in Figure 6 ( $I = 100$  mA, 0.12 mA / bunch, 5% coupling). Given the small currents per bunch, it is assumed that no bunch lengthening occurs and that the usual scaling of zero-current bunch lengths with  $\sqrt{V_{RF}}$  applies for the Touschek contribution.

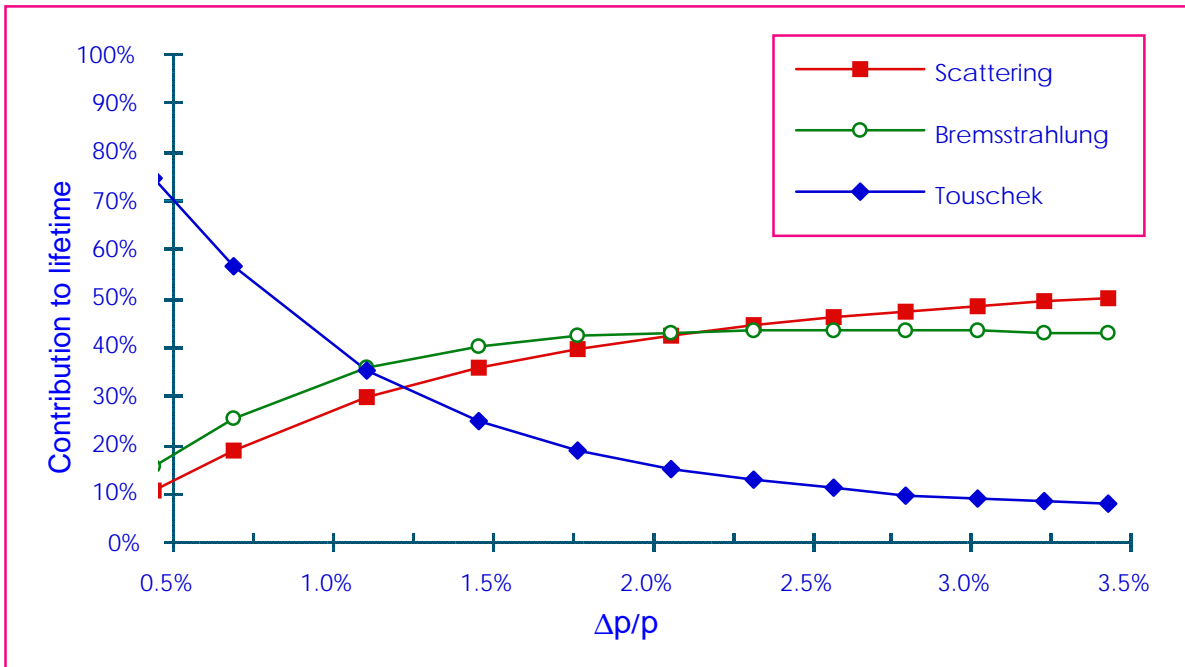


**Figure 6:** Evolution of the different contributions to the lifetime when decreasing the energy acceptance

It can be seen that the contribution of the elastic gas scattering is as large as the Bremsstrahlung one, due to the high scattering rate on the  $\pm 2.5$  mm high ID3 vacuum vessel. Measurements below  $\Delta p/p = 1\%$  (i.e., VRF = 6.4 MV) are not of much use since the Touschek contribution takes over. Decreasing the intensity to 25 mA whilst keeping the large coupling does not significantly help, as shown in Figure 7.

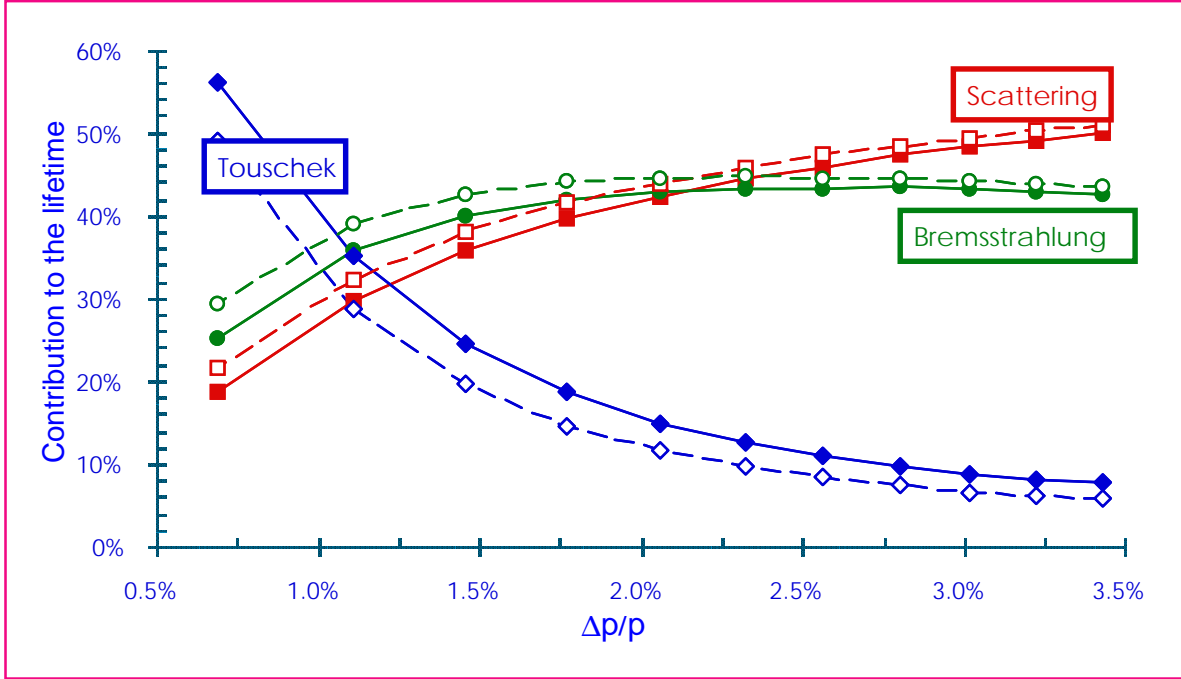


Figure 7: Influence of the intensity (---- I = 25 mA) on the different contributions to the lifetime when decreasing the energy acceptance

### ☞ Touschek:

The Touschek lifetime can be expressed as:

$$\frac{1}{\tau_T} = C_T \frac{N}{\sigma_x \sigma_y \sigma_L \left( \frac{\Delta p}{p} \right)_{\max}^2} f \left[ \sigma_x, \sigma_y, \sigma_E, \left( \frac{\Delta p}{p} \right)_{\max} \right],$$

where  $C_T$  is a constant,  $N$  is the number of particles per bunch,  $\sigma_x$  and  $\sigma_y$  are the transverse beam sizes,  $\sigma_L$  is the bunch length,  $\sigma_E$  is the energy spread, and  $(\Delta p/p)_{\max}$  is the energy acceptance that is determined by either the rf bucket or by transverse limitations (physical or dynamic aperture). Since the only unknown is the energy acceptance (although some assumption on the energy widening has to be made), the strategy consists of recording the lifetime as a function of the rf voltage in single bunch mode and deducing  $(\Delta p/p)_{\max}$  from the fit of the experimental data.

However, simulations with a 5-mA single bunch (assuming a coupling of 1.6%, bunch lengthening of 2.38) show that gas scattering and Bremsstrahlung contributions have to be taken into account (Figure 8).

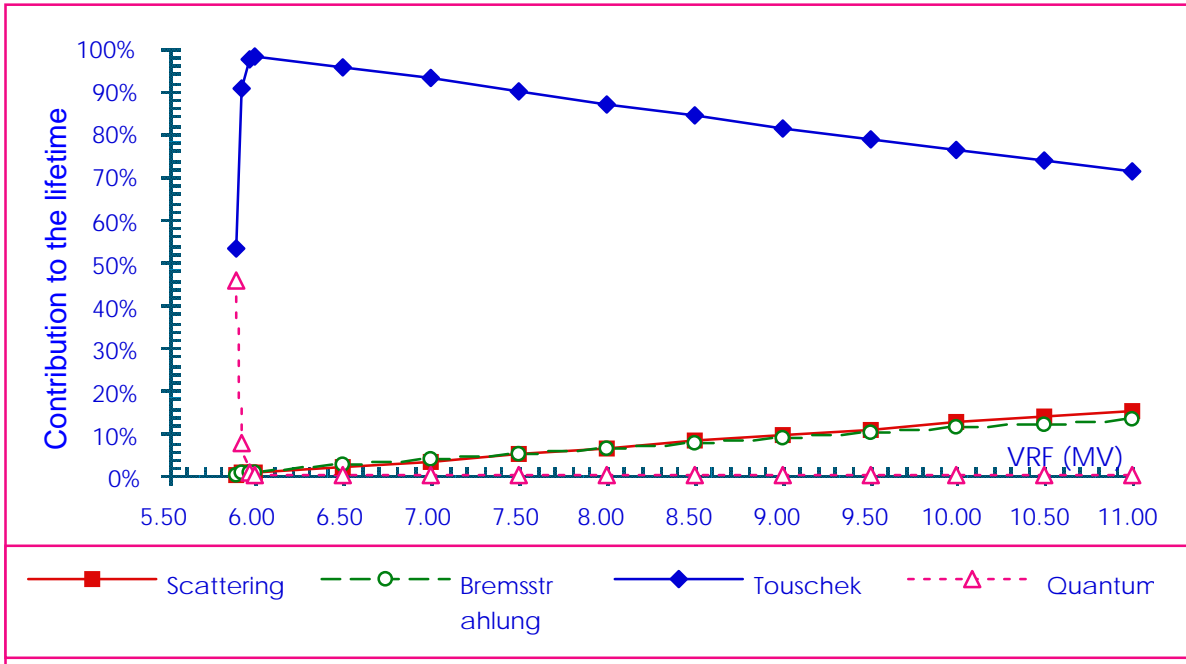


**Figure 8:** Evolution of the different contributions to the lifetime versus rf voltage in single bunch

## Measurements

Experiments were performed with the following conditions:

☞ Sept 7: Gas scattering measurement at 100 mA at the restart of the machine after a power outage and recovery. The desired filling pattern was 83\*10 by 14. However, analysis of the data shows that only 600 buckets were filled (Figure 9), leading to an intensity of 0.17 mA/bunch. The tunes were brought to the coupling resonance (Figure 10) with final values of  $\nu_x = 0.237$ ,  $\nu_y = 0.257$ . No emittance measurement was available due to the power outage. Data are in `sr/daily/9809/07/2/lifetime` and labeled `series01.xxx`. The lifetime was derived by running the `takeDataLifetime` script with a 120 s acquisition time of the S35 DCTT. A very good precision was obtained since the uncertainty on the lifetime was  $\pm 0.28$  h in the worst case.



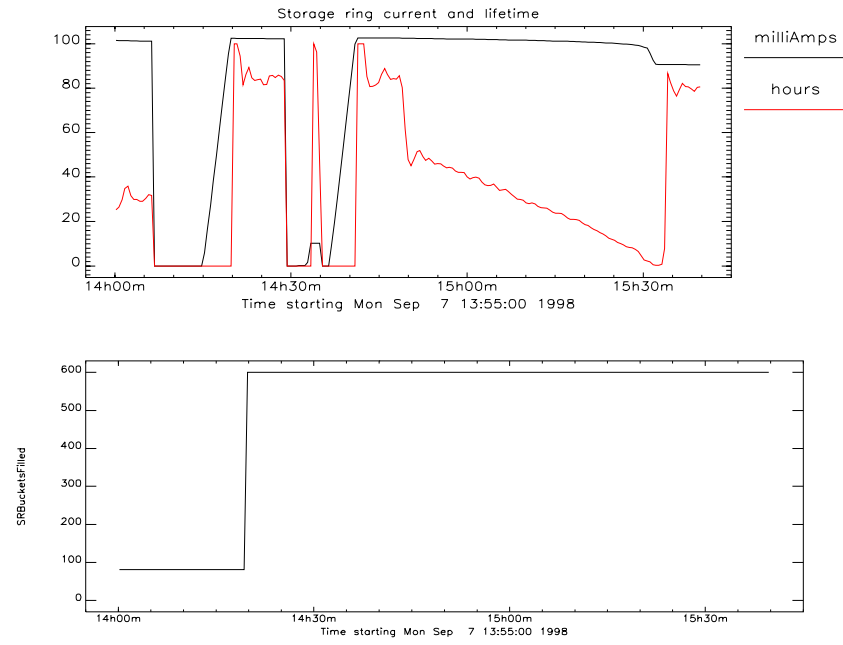


**Figure 9:** Filling pattern, intensity and lifetime during the Sept 07 experiment

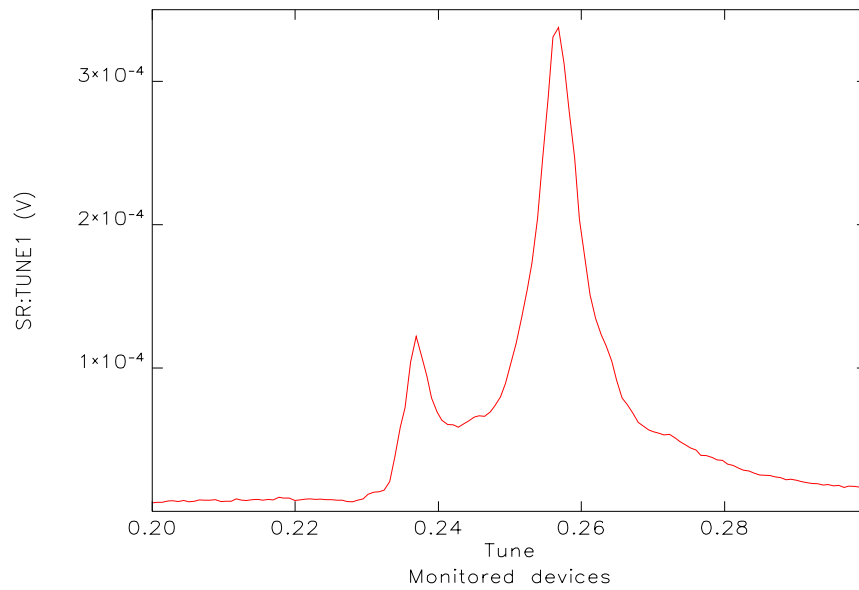


**Figure 10:** Tunes during the Sept 07 experiment

Sept 14: Measurements were carried with a configuration steering the beam to zero vertical setpoints in order to center the beam vertically in the IDs (SR1998-213-0731-103405.gz). Again the filling pattern (83\*10 by 14) defined for the gas scattering experiment was not achieved. This was due to the fact that while the injector was running at full current, the injection was suspended to avoid tripping by the radiation monitors. When injection resumed with the same bucket numbers, a non-uniformly filled 395 bucket pattern was obtained (Figure 11). However, given the small contribution from Touschek lifetime in the experiment, this only had a marginal impact on the results.

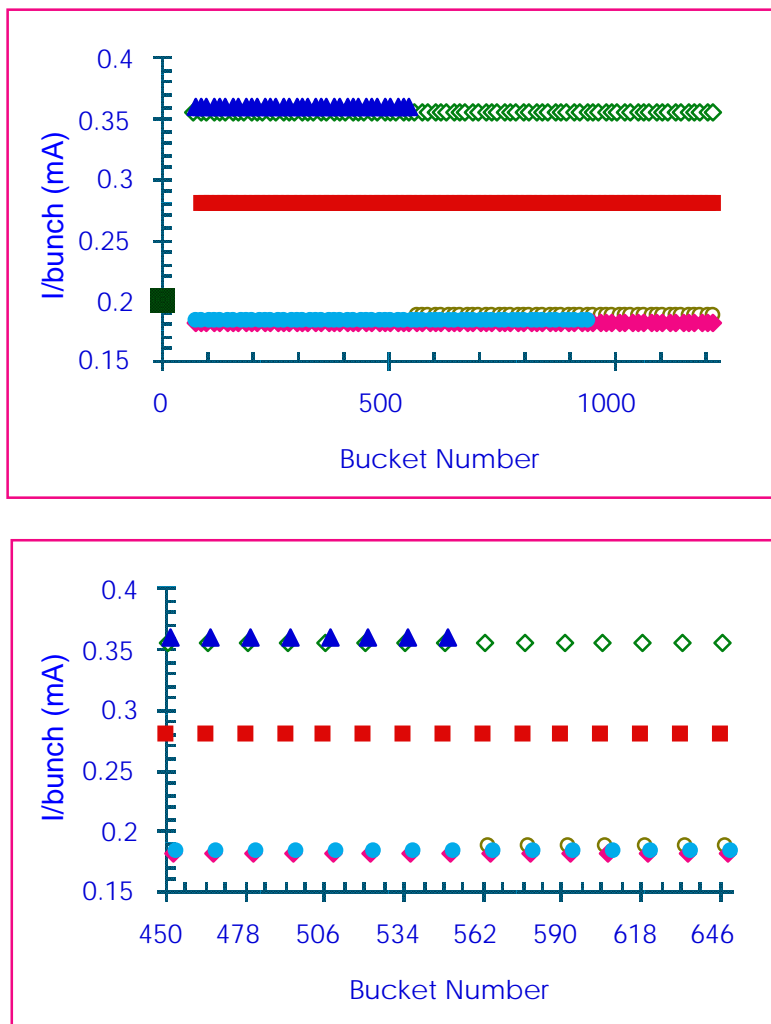


Figure 11: Filling pattern (total and zoom) for gas scattering measurements

With this filling pattern, the beam characteristics at 100 mA were the following:

$$\begin{aligned} \epsilon_x &= 9 \text{ nm} & \nu_x &= 0.212 \\ \epsilon_y &= 0.2 \text{ mm} & \nu_y &= 0.271 \\ \text{coupling} &= 2.2\% \end{aligned}$$

The tunes were brought to the coupling resonance for the gas scattering experiment (Figure 12), which lead to the following characteristics:

$$\begin{aligned} \epsilon_x &= 7.5 \text{ nm} & \nu_x &= 0.256 \\ \epsilon_y &= 0.47 \text{ mm} & \nu_y &= 0.271 \\ \text{coupling} &= 6.6\% \end{aligned}$$

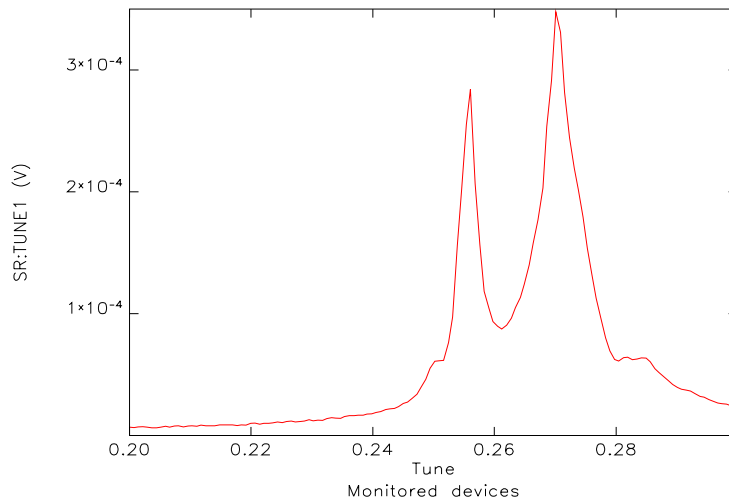


**Figure 12:** Tunes during the Sept 14 experiment

Three sets of data (lifetime versus S38 top scraper position) were taken at 100 mA, and then at 50 mA and 20 mA after scraping the beam (Figure 13). The data are in sr/daily/9809/15/1 and are labeled LifetimeSeries.xxx, LifetimeSeries\_50mA.xxx, LifetimeSeries\_25mA.xxx.

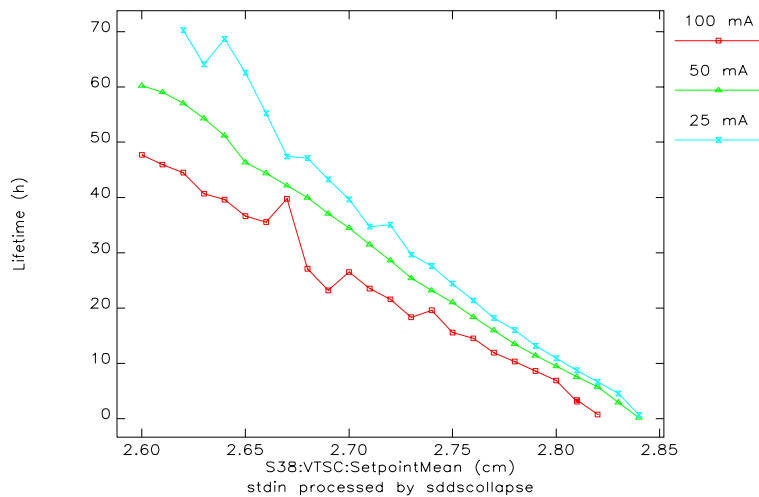


**Figure 13:** Lifetime versus scraper position

As shown in Figure 14, a noticeable evolution of emittances was observed between 100 mA and 50 mA with the coupling decreasing to 4.9%. This does not seem to be due to a motion of the beam (there was no orbit correction during the scraper measurements because of the filling pattern) since the beam centroid was drifting linearly (Figure 15). Also the tunes remained unchanged with respect to the values at 100 mA (Figure 16).

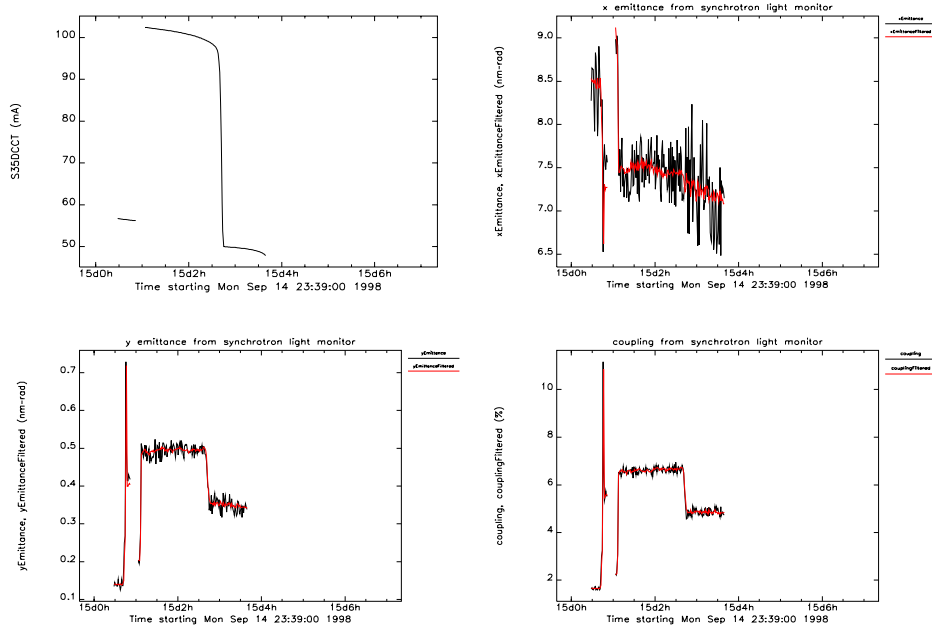


**Figure 14:** Emittance evolution during the gas scattering experiment

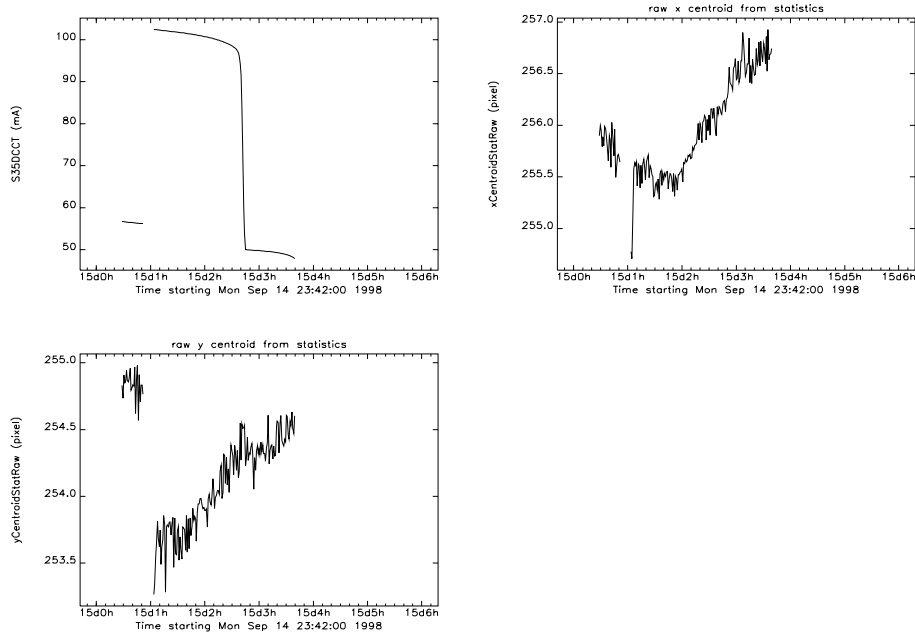


**Figure 15:** Motion of the raw beam image centroid during the gas scattering experiment

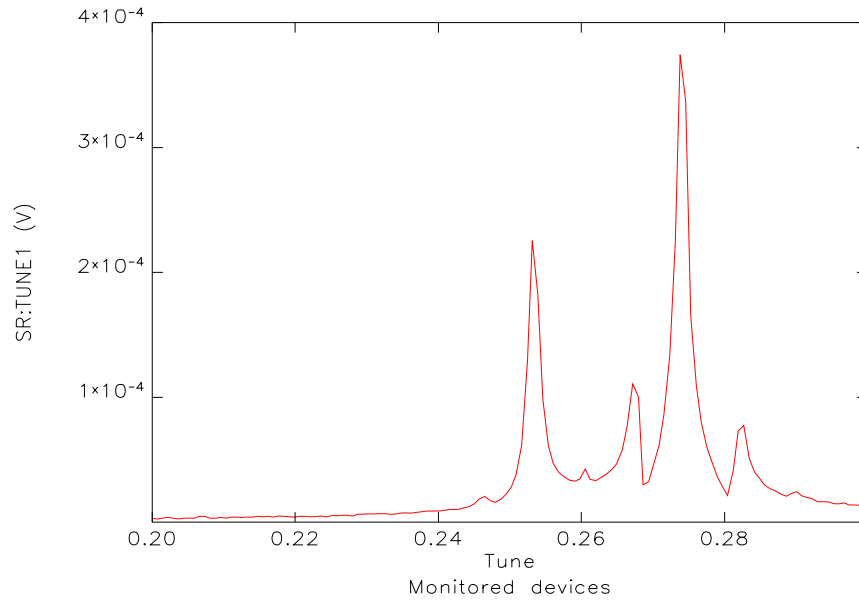


**Figure 16:** Tunes at 50 mA

After having restored the nominal tunes, the Touschek experiment was performed with filling the machine with a 5.4-mA single bunch. The emittance measuring device was set up for standard 100-mA beam, and therefore no emittance data could be recorded. However, since the vertical tune shift with intensity brought the tunes closer to each other ( $\nu_x = 0.2045$ ,  $\nu_y = 0.2598$ ), the coupling could be higher than for the 100-mA beam. The lifetime was recorded versus the rf voltage, starting from 11 MV. Data are found in sr/daily/9809/15/1 and are labeled SingleBunchLifetime.xxx. For most of the data, the acquisition time was set at 300 s in the takeDataLifetime script in order to improve the precision (Figure 17).

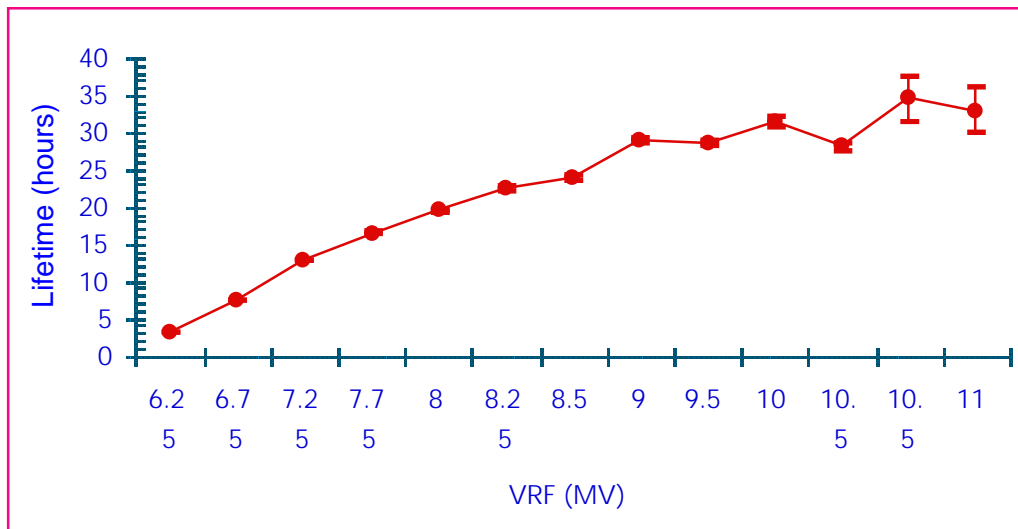


**Figure 17:** Single bunch lifetime versus rf voltage

☞ Sept 21: The objective of the studies was to assess the lifetime model derived from the previous experiments by filling the machine with various filling patterns and recording the lifetime at 100, 75, 50, and 25 mA. The configuration SR1998-213-0731-103405.gz, which centers the beam vertically in the IDs, was used. As shown in Figure 18, the filling patterns were the following:

- 83 \* 10 buckets with an interval of 14 buckets
- 83 \* 2 buckets with an interval of 14 buckets
- 25 \* 3 buckets with an interval of 32 buckets
- 22 \* 1 buckets with an interval of 52 buckets

The beam decay was simulated by scraping the beam with the S38 top scraper (set in the 2.8 - 2.9 cm range) except on a few occasions where the scraping was too fast and the beam lost. The desired intensity was then obtained by refilling the machine.

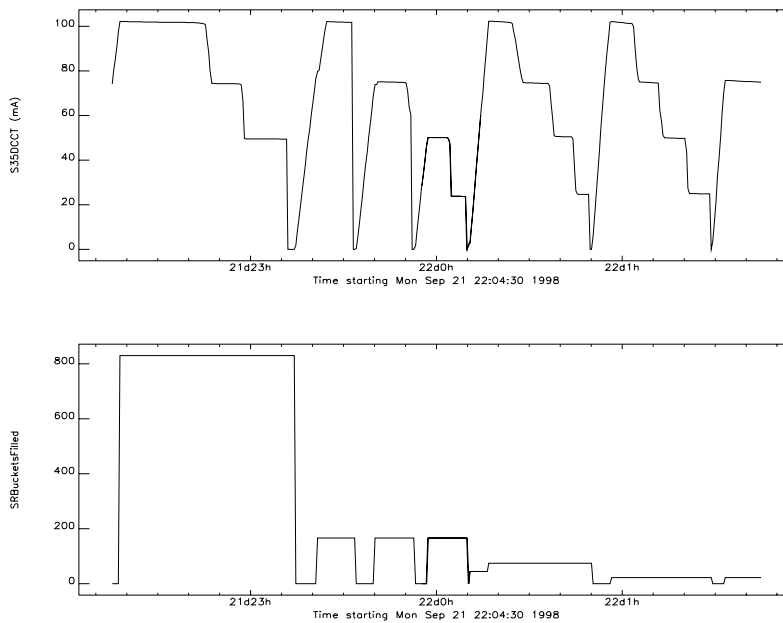
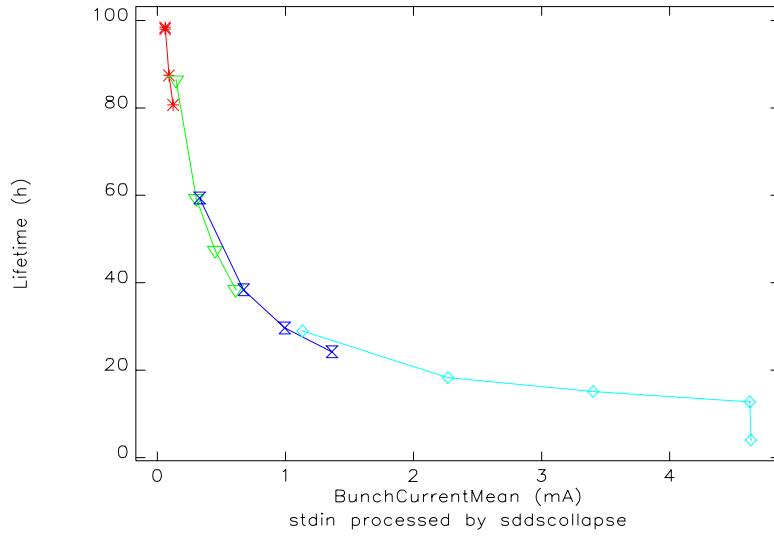


Figure 18: Filling patterns during the Sept 21 experiment

Lifetimes were obtained by running the takeLifetimeData script with a minimum current change of 0.1 mA and a maximum data collection time of 200 s in most cases (0.2 mA and 300 s for the 22 \* 1 by 52 filling pattern). Data are found in /home/helios/SR/daily/9809/21/3/LifeTime and are labeled series0X.xxx. They are plotted in Figure 19.



**Figure 19:** Lifetime dependence on intensity/bunch

Emittance and tune evolution are given in Table 3. The reasons for the large horizontal emittance initially recorded with the 83 \* 10 filling pattern are unclear (this was not observed during the former experiment). On the other hand, the beam was clearly excited horizontally at 100 mA in the 22 \* 1 pattern. The chromaticities, as measured by the previous team, were:  $\xi_x = 0.96 \pm 0.45$ ,  $\xi_y = 3.6 \pm 0.12$ .

**Table 3**

filling pattern	I (mA)	$\nu_x$	$\nu_y$	$\epsilon_x$ (nm)	$\epsilon_y$ (nm)	$\kappa$ (%)
83 * 10	101.8	0.2022	0.2753	10.7	0.13	1.2
	74.3	0.2	0.2753	8.6	0.107	1.2
	49.5	0.1993	0.2767	7.8	0.1	1.2
83 * 2	102	0.2	0.2723	9.14	0.1	1.25
	75.1	0.1995	0.2746	8.5	0.11	1.2
	50.1	0.1985	0.2753	8.1	0.097	1.2
	23.8	0.1963	0.276			
25 * 3	102.2	0.1986	0.2686	9.1	0.11	1.2
	74.5	0.1985	0.2649	8.7	0.11	1.3
	50.5	0.1977	0.2753	7.7	0.1	1.1
	24.7	0.197	0.276			
22 * 1	101.9	0.197	0.262	12.6	0.125	0.94
	74.8	0.1956	0.2664	10.5	0.114	1.1
	49.9	0.1963	0.2686	8.2	0.09	1.14
	24.9	0.197	0.2694			

The lifetime was also recorded at a single intensity (75 mA) after having moved the tunes to the coupling ( $\nu_x = 0.249$ ,  $\nu_y = 0.265$ ), but surprisingly the coupling increased very little (1.5%).

☞ Sept 27: The gas scattering experiment was reproduced with a smaller rf gap voltage (8 MV instead of the standard 9.4 MV) to see whether a reduced energy acceptance would have some effect on the gas scattering loss rate. Again the machine was filled with the 83 \* 10 by 14 bunch pattern (the 830 buckets were effectively filled) and measurements carried at 100 mA and 50 mA with the configuration centering the beam vertically in the IDs. A large horizontal emittance (12.65 nm) was initially recorded with tunes at  $\nu_x = 0.2066$ ,  $\nu_y = 0.2752$  whilst the coupling was standing at 1.2% ( $\epsilon_y = 0.15$  nm). Surprisingly, no vertical emittance increase was obtained after having moved the tunes towards the coupling ( $\nu_x = 0.25$ ,  $\nu_y = 0.272$ ).

During the ramping of the rf voltage down to 8 MV, a transient dramatic excitation of the beam in the horizontal plane could be observed. After damping of the instability, the following emittances were measured:  $\epsilon_x = 10.76$  nm,  $\epsilon_y = 0.145$  nm, coupling = 1.35%. Apparently the significant increase of the horizontal emittance in this filling pattern comes from an instability induced blow-up since a standard figure was retrieved at 50 mA (but with still a low coupling):  $\epsilon_x = 7.9$  nm,  $\epsilon_y = 0.09$  nm, coupling = 1.19%.

The lifetime was recorded versus S38 top scraper position using the takeLifetimedata script (with a 120 s maximum data collection time). Data can be found in sr/daily/9809/27/2/Lifetime and are labeled Series100mA.xxx and Series50mA.xxx. Figure 20 gives a comparison of the raw lifetime data versus scraper position recorded during the different experiments at 100 mA. The scraper range seems to extend to smaller apertures when the rf voltage is reduced.



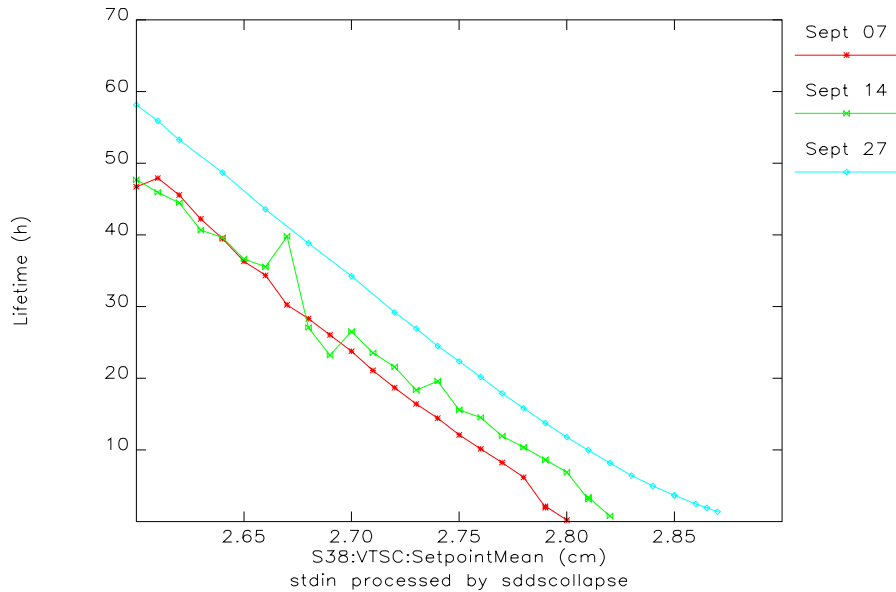


Figure 20: Comparison of raw lifetime data at 100 mA for the three gas scattering experiments

### **Analysis of gas scattering data**

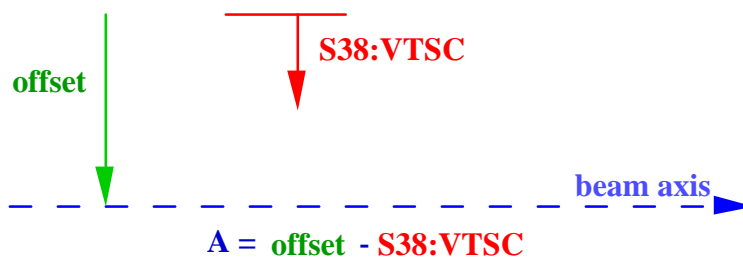
The data was analyzed using two methods.

☞ The first method fit the raw data to the expected lifetime computed from simulations.

The following assumptions are taken for computing the different lifetimes:

- Touschek:*
- measured transverse beam emittances
  - energy acceptance deduced from the Touschek experiment
  - intensity/bunch taken from the highest filled bucket
  - theoretical bunch length and energy widening

*Gas scattering:* the lifetime depends on the average pressure P (the gas composition is taken from Table 1) and the position A of the scraper with respect to the beam axis. Since the measured scraper position (S38:VTSC) is related to an external reference, an offset is introduced as a free parameter as sketched below.



*Bremsstrahlung:* the energy acceptance and pressure determined above are used for the Bremsstrahlung lifetime.

The results of the fit are given in Figure 21 and Table 4.

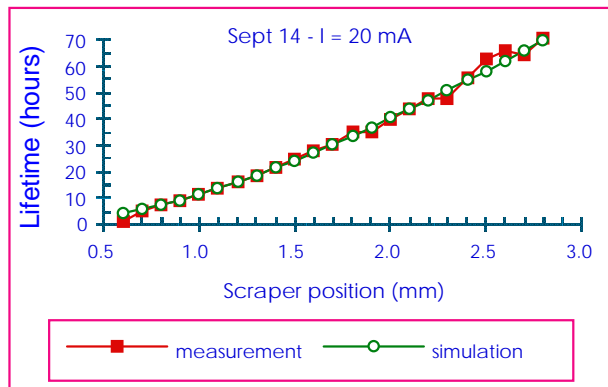
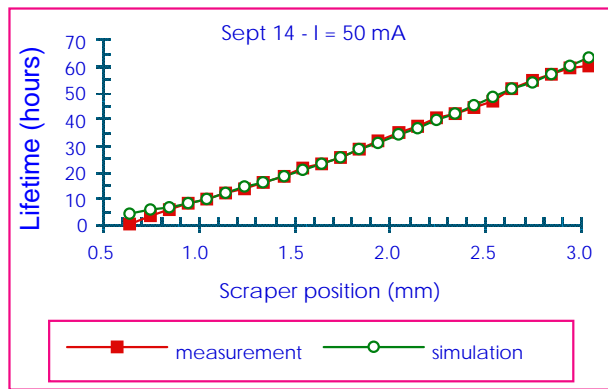
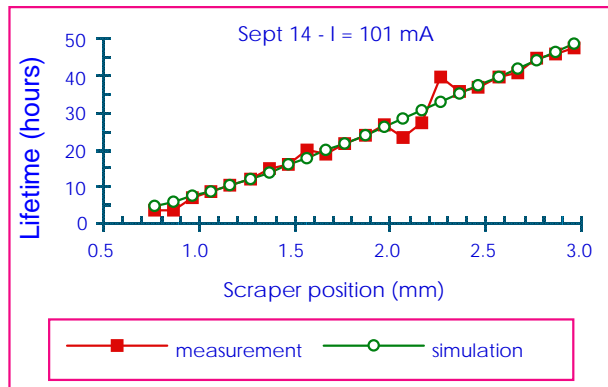
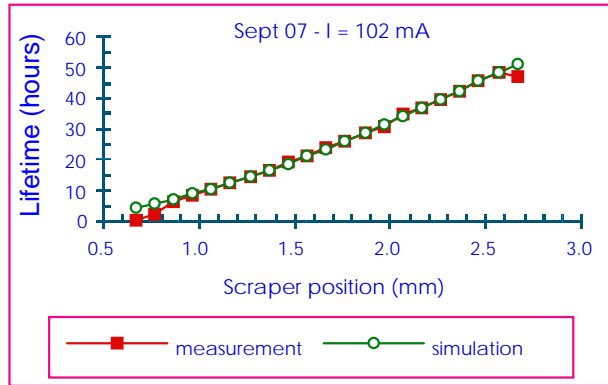


Figure 21: Fit of the lifetime versus scraper measurements

Table 4

	I = 102 mA Sept 7	I = 101 mA Sept 14	I = 50 mA Sept 14	I = 20 mA Sept 14
average pressure (nT)	0.497	0.577	0.484	0.403
scraper offset (mm)	28.67	28.97	29.045	29.005

On average (there are a few erratic measured lifetimes), the agreement between the measurements and the simulations is very good. However, in the quantum region, the lifetime decreases more rapidly than predicted. The differences between the Sept 7 and Sept 14 fits at 100 mA are likely due to the fact that, after a long shutdown, the machine was not yet in a steady state on Sept 7. For the Sept 14 fits at different intensities, the peak difference of 75  $\mu\text{m}$  in scraper offsets could be due to an orbit drift, since no correction was applied.

If one assumes that the pressure dependence on the intensity is given by the following law  $\bar{P} = P_0 + \frac{\partial P}{\partial I} I$ , the static pressure  $P_0$  and the coefficient  $\frac{\partial P}{\partial I}$  can be estimated from the gas scattering fits as shown in Figure 22.

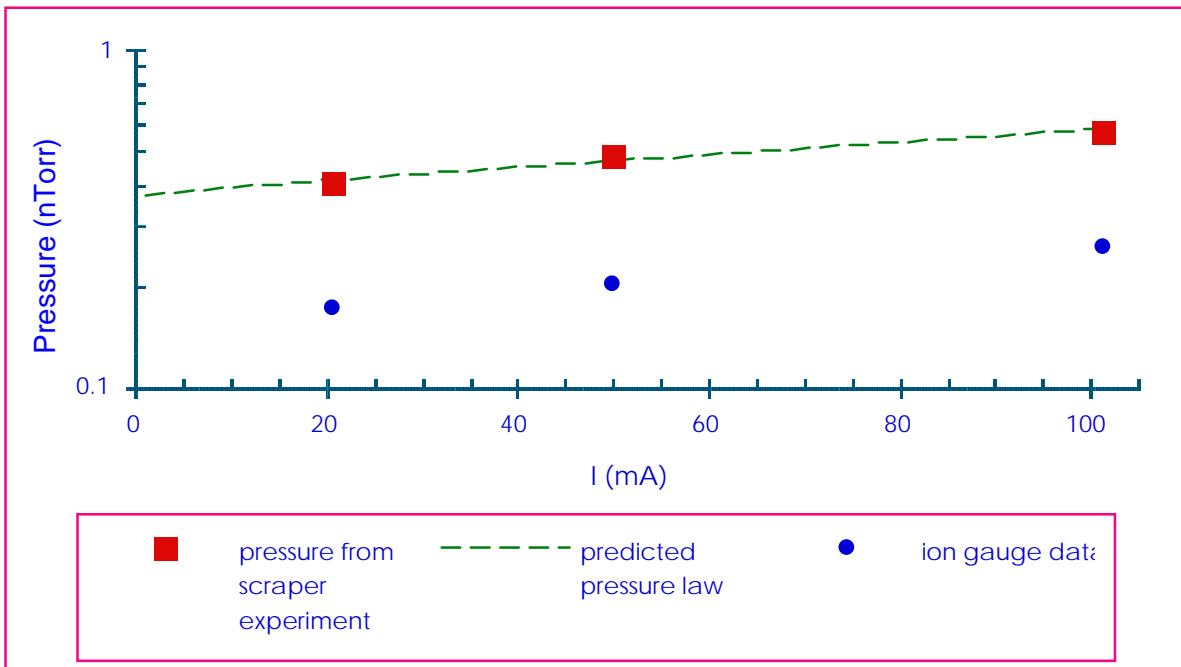


Figure 22: Predicted pressure law with  $P_0 = 0.367 \text{ nT}$ ,  $\frac{\partial P}{\partial I} = 2.11 \cdot 10^{-3} \text{ nT} / \text{mA}$

It has to be noted that the predicted pressure is higher than the readings from ion gauges (which give underestimated values due to their location in the antechamber). Also, the readings of ion pumps (see Figure 23) do not reflect the real pressure seen by the beam.

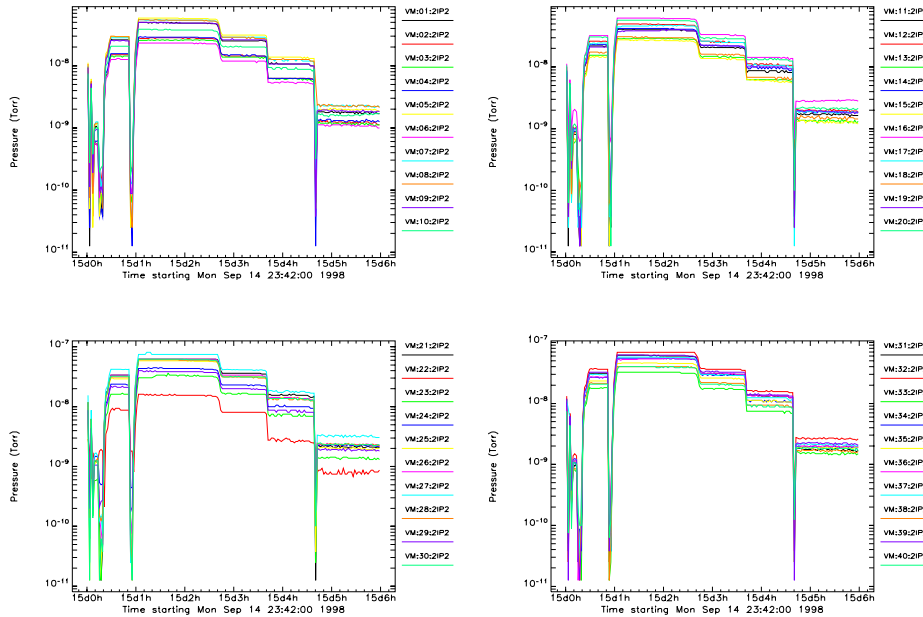


Figure 23: Pressure readings from a set of ion pumps during the gas scattering experiment

Although the gas scattering contribution is the dominant one, incorrect assumptions in the computed Touschek lifetime may alter the results of the previous fitting method. As an example, Figure 24 gives the changes in the predicted pressure law when the Touschek lifetime changes.

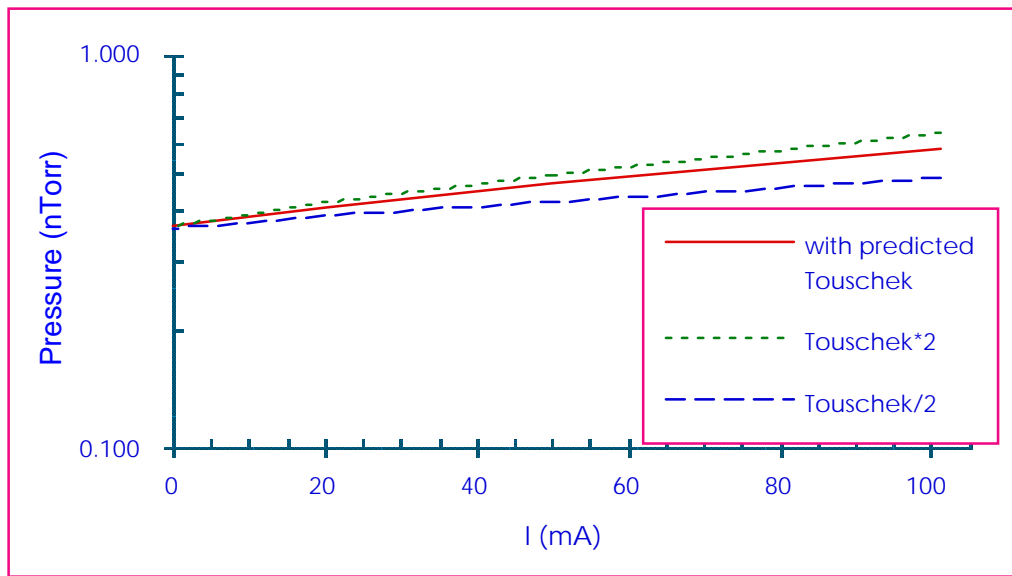


Figure 24: Uncertainties of the predicted pressure law

☞ In order to overcome the drawbacks of the previous fitting method, the second method only assumes that the Bremsstrahlung and Touschek contributions ( $\tau_B$  and  $\tau_T$ ) remain constant during the scraper scan at a given intensity. This is realistic since no variations in pressure, acceptance in energy, or emittances should occur. Under these conditions, the curve  $\frac{I}{\tau_{meas}} = b + \frac{I}{\tau_G} = b + \frac{a}{A^2}$ , where  $b = \frac{I}{\tau_B} + \frac{I}{\tau_T} = \text{Constant}$  should be linear with respect to  $A^{-2}$  (A being the scraper aperture). Figure 25 shows the results of the fit of the coefficients  $a$  and  $b$  for the different measurements.

Since the expression  $\frac{a}{A^2}$  gives the gas scattering loss rate for the limiting aperture A defined by the scraper, it is easy to find the gas scattering loss rate in normal aperture conditions. It is given by:  $\frac{I}{\tau_G} = \frac{\beta_{ID3}}{\beta_A} \frac{a}{A_{ID3}^2}$ , where  $\beta_{ID3}$  is the vertical  $\beta$  function at the end of the ID3 straight section ( $\beta_{ID3} = 6.76$  m), and  $A_{ID3}$  is the vertical half-aperture of the vacuum vessel ( $A_{ID3}=2.5$  mm). However, errors in the determination of the scraper offset result in different linear dependences of the measured lifetime on  $A^{-2}$  and different loss rates. Figure 26 shows the dependence of the fit of the linear law on the offset value. The quality of the fit is expressed in terms of  $\chi^2$  where:

$$\chi^2 = \sum_{meas} \left[ \frac{1}{\tau_{meas}} - \left( b + \frac{a}{A^2} \right) \right]^2.$$

The corresponding error bars (when considering a  $\pm 0.1$  mm uncertainty on the scraper offset) for the evolution of the elastic gas scattering loss rate with intensity are given in Figure 27. The approximation to a linear dependence is shown in Figure 28. The elastic gas scattering loss rate can be estimated at:

$$\frac{I}{\tau_G} = 1.7510^{-5} \text{ hours}^{-1} . \text{mA}^{-1} \text{ with an error of } 0.2 \text{ hours}^{-1} . \text{mA}^{-1}$$

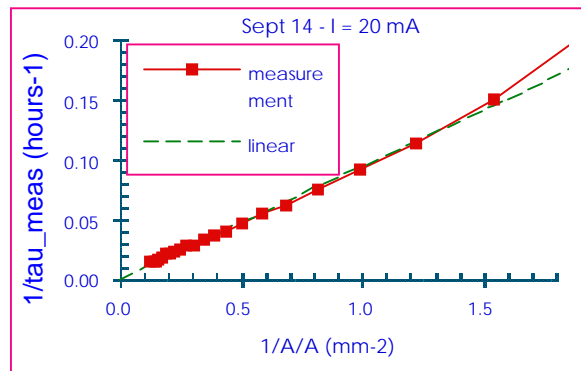
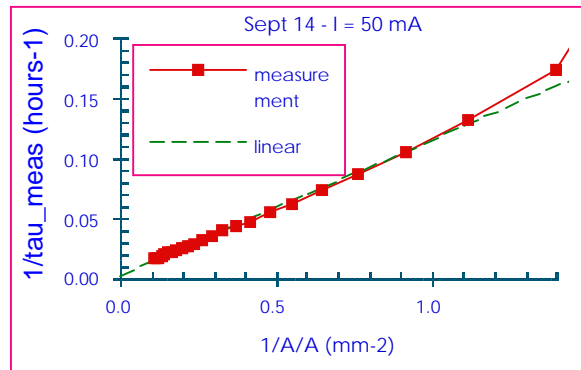
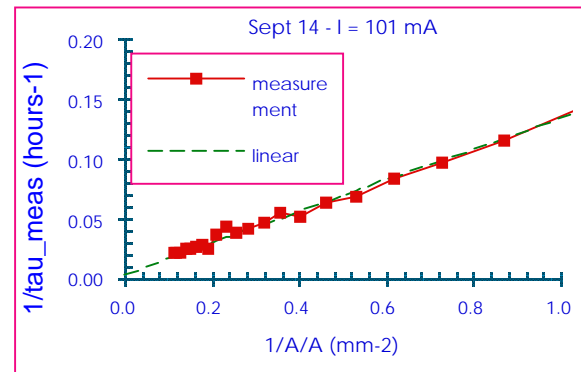
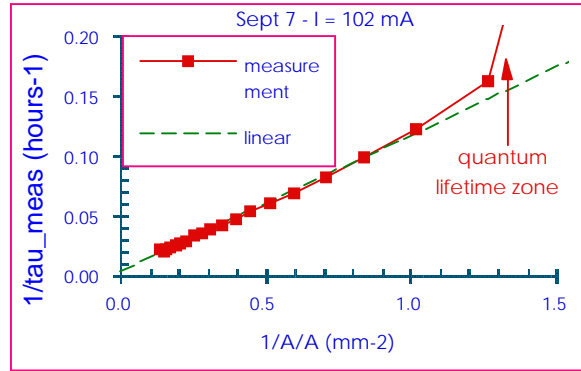


Figure 25: Linear dependence of  $\frac{1}{\tau_{meas}}$  on  $\frac{1}{A^2}$

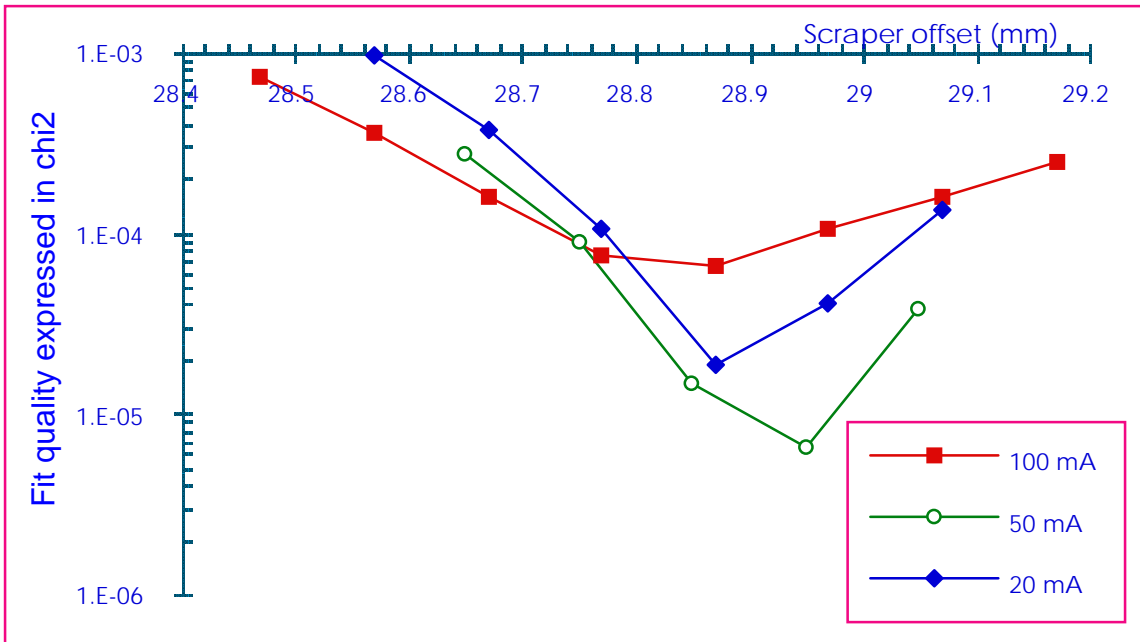


Figure 26: Dependence of the fit on the scraper offset

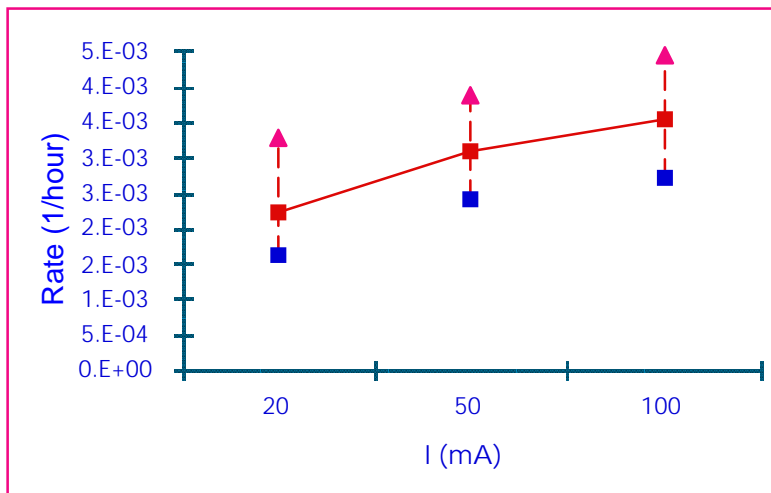


Figure 27: Loss rate as a function of current

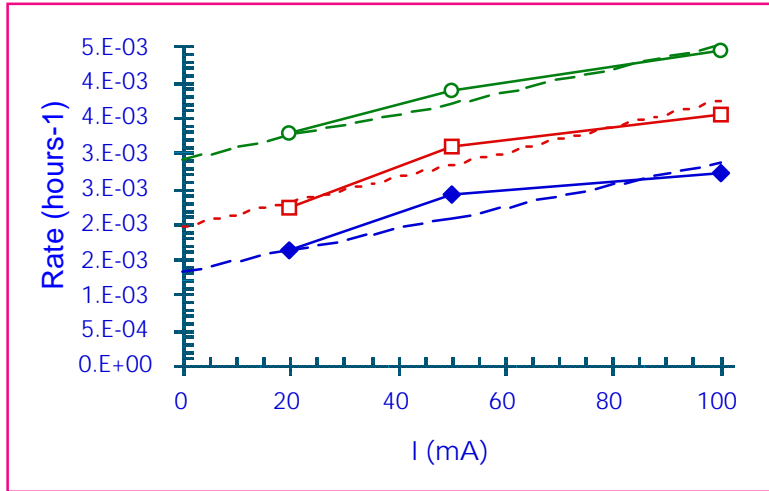


Figure 28: Linear approximation for the loss rate as a function of current

### **Analysis of the Touschek lifetime measurement**

As shown in Figure 29, the measured lifetime increases, as expected, with the rf voltage and the bucket height  $\frac{\Delta p}{p}$  up to about 9 MV. The asymptotic behaviour for higher voltages clearly demonstrates that the energy acceptance is no longer dictated by the rf voltage above 9 MV but that the limitation comes from transverse considerations. This leads to an energy acceptance of the order of 2.5%.

The results of computation of the lifetime in the zone where the energy acceptance is determined by the rf voltage are also plotted in Figure 29. The Touschek contribution is computed with the following assumptions:

- same transverse emittances as for a standard fill ( $\epsilon_x = 8.5$  nm,  $\epsilon_y = 0.139$  nm)
- bunch lengthening of 2.38 at any rf voltage extrapolated from the measurement at 11 MV performed on Aug 31 (see Figure 30). An excellent agreement was obtained between measured bunch lengths and the expected dependence of the bunch length with current given by:

$$\sigma^3 - \sigma = I \frac{8\eta}{9\pi^2 \sqrt{2\pi} \sigma_{L_0}^3 E v_s^2} \text{Im}\left(\frac{Z_{\parallel}}{n}\right),$$

where  $\sigma = \frac{\sigma_L}{\sigma_{L_0}}$ ,  $\sigma_L$  and  $\sigma_{L_0}$  are the bunch lengths at  $I$ , and  $I = 0$ ,  $v_s$  is the synchrotron

frequency,  $E$  is the machine energy, and  $\frac{Z_{\parallel}}{n}$  is the longitudinal impedance

- no energy widening is considered (in any case, it plays a marginal role)



- number of particles/bunch scaled with the intensity

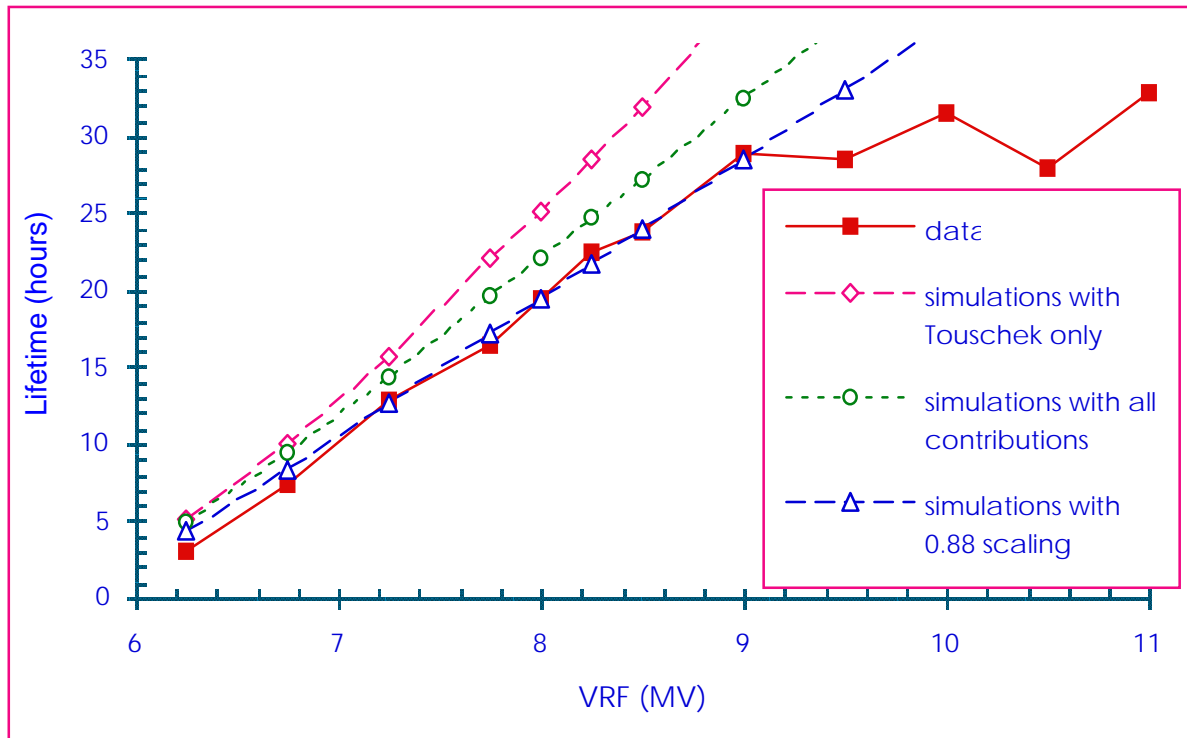


Figure 29: Modeling of the single bunch lifetime

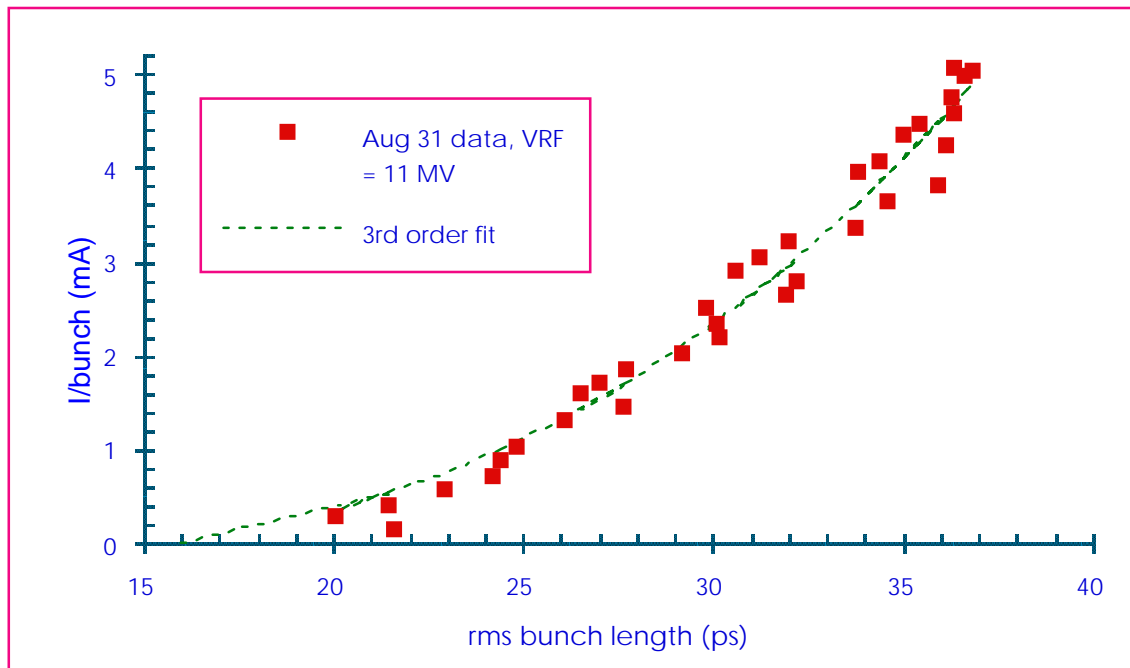


Figure 30: Third-order fit of measured bunch lengths

A significant discrepancy with respect to the measured lifetime is observed. This can be reduced by introducing the expected gas scattering contributions. As mentioned earlier, although the lifetime is Touschek dominated in single bunch, the other contributions to the lifetime must be taken into account. In these conditions, the agreement between simulations and measurements is excellent, provided a scaling factor of 0.88 is applied to the computed lifetime. This could mean that some of the measured beam sizes are overestimated, for instance by 14% for the bunch length or 28% for the vertical emittance. Bunch length measurements at very small current could possibly assess the assumption of an overestimation from the streak camera, although it could be difficult to distinguish between bunch lengthening and measuring errors due to the small current.

### **Analysis of the lifetime dependence on filling patterns**

The objectives of the measurements were twofold:

- check the credibility of the lifetime model derived from the previous measurements
- derive from the lifetime comparison at the same intensity the gas scattering rates (elastic and inelastic)

Figure 31 shows a comparison of the measured lifetimes for the different filling patterns. The evolution, together with the evolution shown in Figure 19, suggests that the Touschek contribution is the dominant one since, at a given total current, the differences in lifetime between the different filling patterns must be attributed to the intensity/bunch lifetime dependence, i.e., to the change in Touschek lifetime. It is assumed that no outgassing and pressure related evolution occur when the intensity/bunch increases.

Expected lifetimes were computed with using the model derived from the previous measurements (pressure law, scaled bunch lengths, energy acceptance). In addition, the measured transverse emittances were used. The results plotted in Figure 32 show that computed lifetimes are significantly larger than measured ones. The discrepancy can be decreased by reducing the energy acceptance from 2.5% down to 1.7%. Whether the energy acceptance is smaller than previously measured (multibunch modes? operating conditions?) has to be assessed.

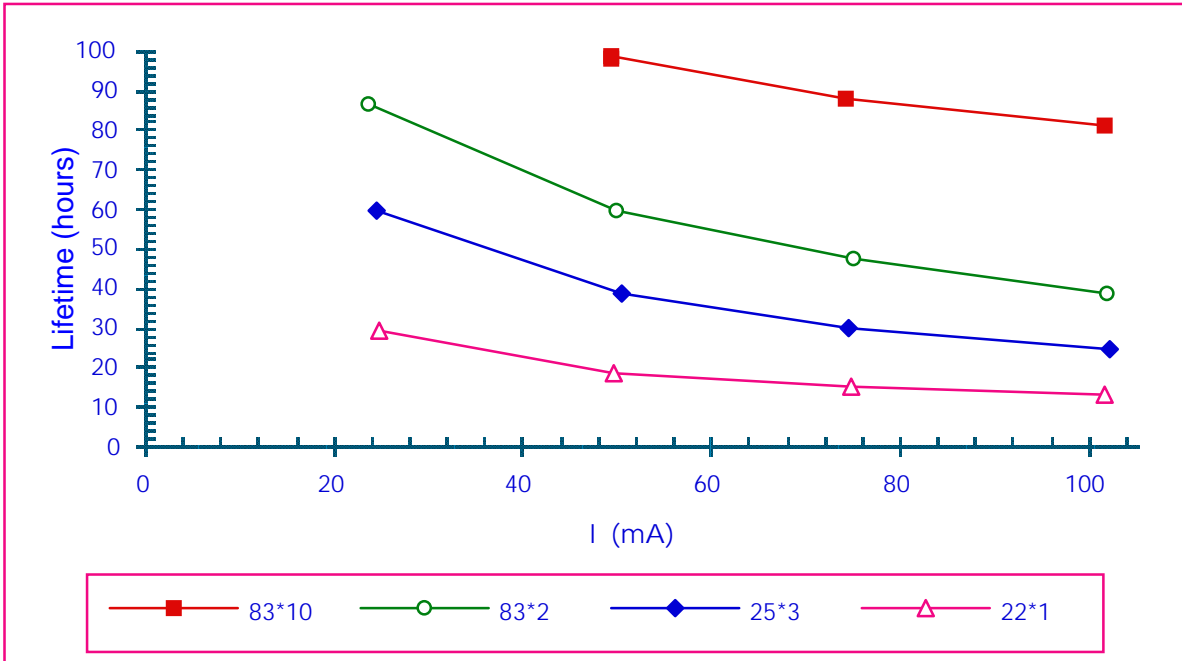


Figure 31: Lifetime dependence on filling patterns

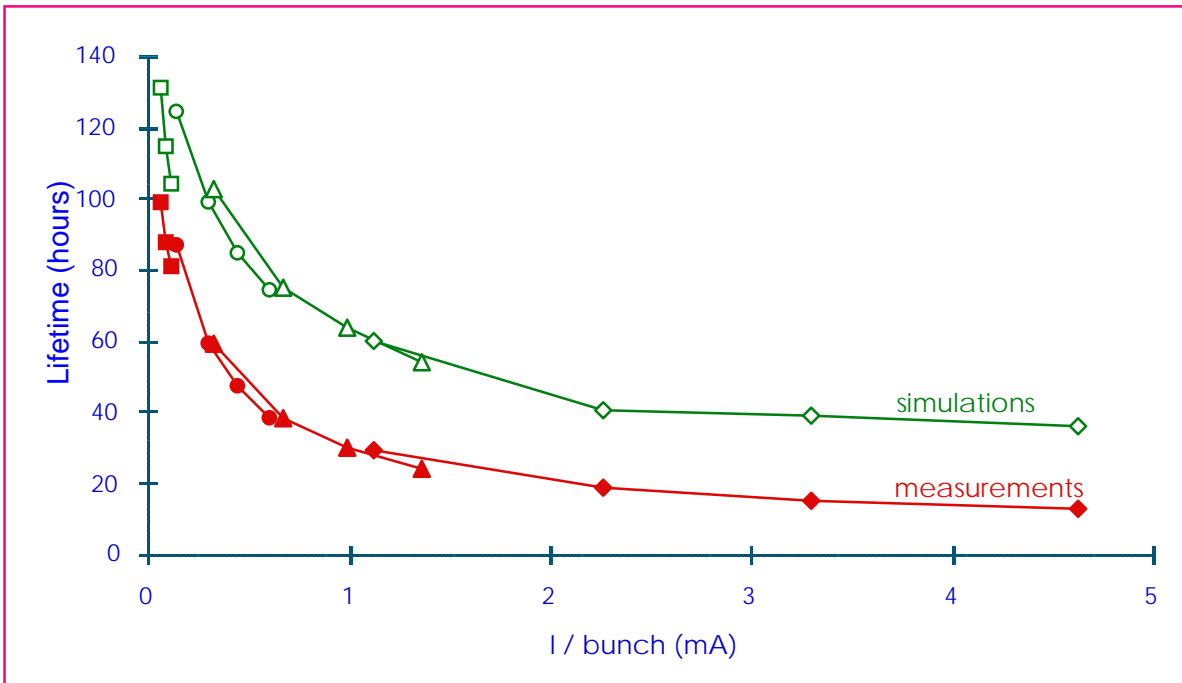


Figure 32: Comparison of measurements and simulations

Since the assumptions of a constant gas scattering ( $\tau_G$ ) and Bremsstrahlung ( $\tau_B$ ) contributions at a given intensity, whatever the filling pattern is, look reasonable, one can write:

$$\frac{1}{\tau} = \frac{1}{\tau_G} + \frac{1}{\tau_B} + \frac{1}{\tau_T} = a + \frac{1}{\tau_T},$$

where  $a$  is a constant and  $\tau_T$  is the Touschek lifetime.

Then, by using the dependence of  $\frac{1}{\tau_T}$  on the intensity per bunch,

$$\frac{1}{\tau_T} = C \frac{I_{bunch}}{\sigma_L(I_{bunch})},$$

and the dependence on the bunch length on the intensity per bunch,

$$\left[ \frac{\sigma_L(I_{bunch})}{\sigma_L(I_{bunch}=0)} \right]^3 - \frac{\sigma_L(I_{bunch})}{\sigma_L(I_{bunch}=0)} = KI_{bunch},$$

one can fit the measured lifetimes to an analytical expression given by

$$\frac{1}{\tau} = a + bI_{bunch}^{2/3},$$

where  $a$  is the gas scattering loss rate.

The results of the fit are excellent. They are shown in Figure 33, and the resulting loss rates versus intensity are plotted in Figure 34.

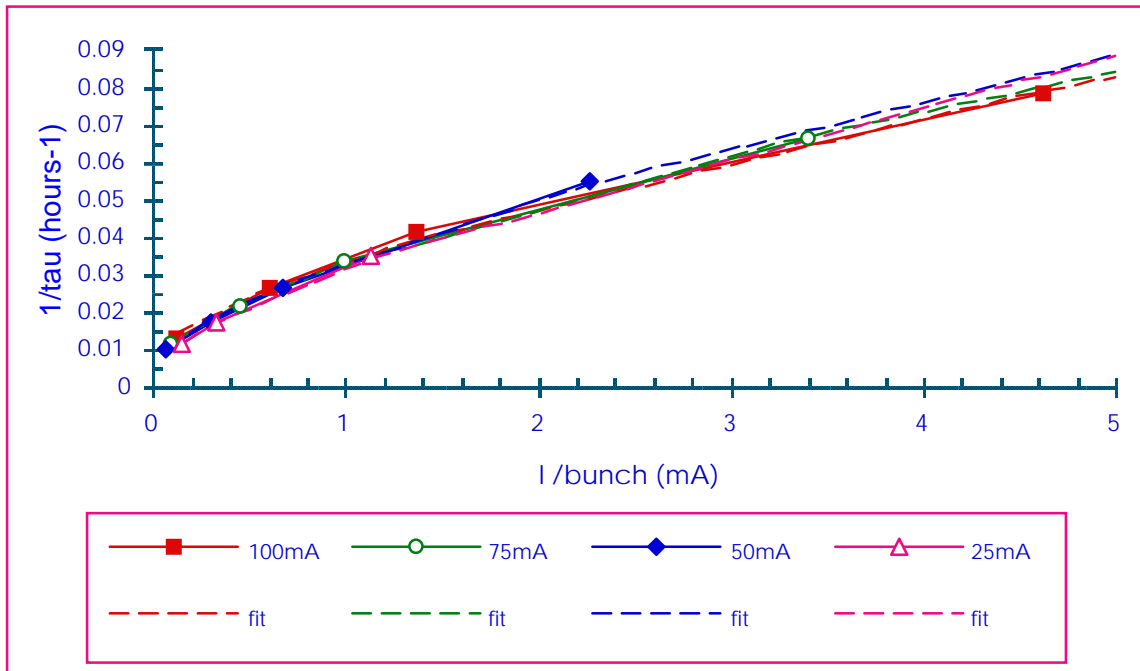


**Figure 33:** Fit of the lifetime to a  $I^{2/3}$  law

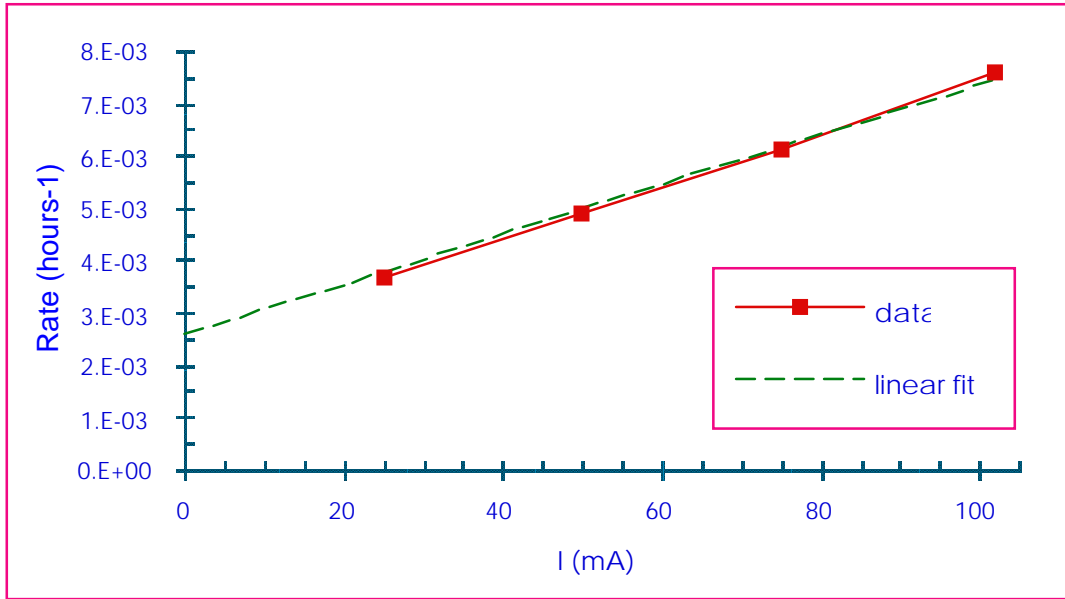


Figure 34: Loss rate versus intensity

The elastic and inelastic gas scattering loss rate can be estimated at

$$\frac{I}{\tau_G} + \frac{I}{\tau_B} = 4.7510^{-5} \text{ hours}^{-1} \cdot \text{mA}^{-1} .$$

This figure is to be compared to previous findings (APS Studies Logbook, 080298-2), summarized in Table 5. There is a good agreement with the third set of values, which was obtained in conditions rather similar to the present ones.

Table 5

Experimental conditions	$\frac{I}{\tau_G} + \frac{I}{\tau_B} (\text{hours}^{-1} \cdot \text{mA}^{-1})$
100 mA in 6+18*3 with high and low coupling	$\leq 7.07 \cdot 10^{-5}$
constant I per bunch for different filling patterns	$8.07 \cdot 10^{-5}$
constant total current	$4.98 \cdot 10^{-5}$

## Gas scattering experiment with reduced rf voltage

The goal was to assess the possible effects of a reduced acceptance in energy and related horizontal-vertical nonlinear coupling on the gas scattering rates. The results of the fits of the measured lifetimes via the two methods previously described are gathered in Figures 35 and 36 and in Table 6.

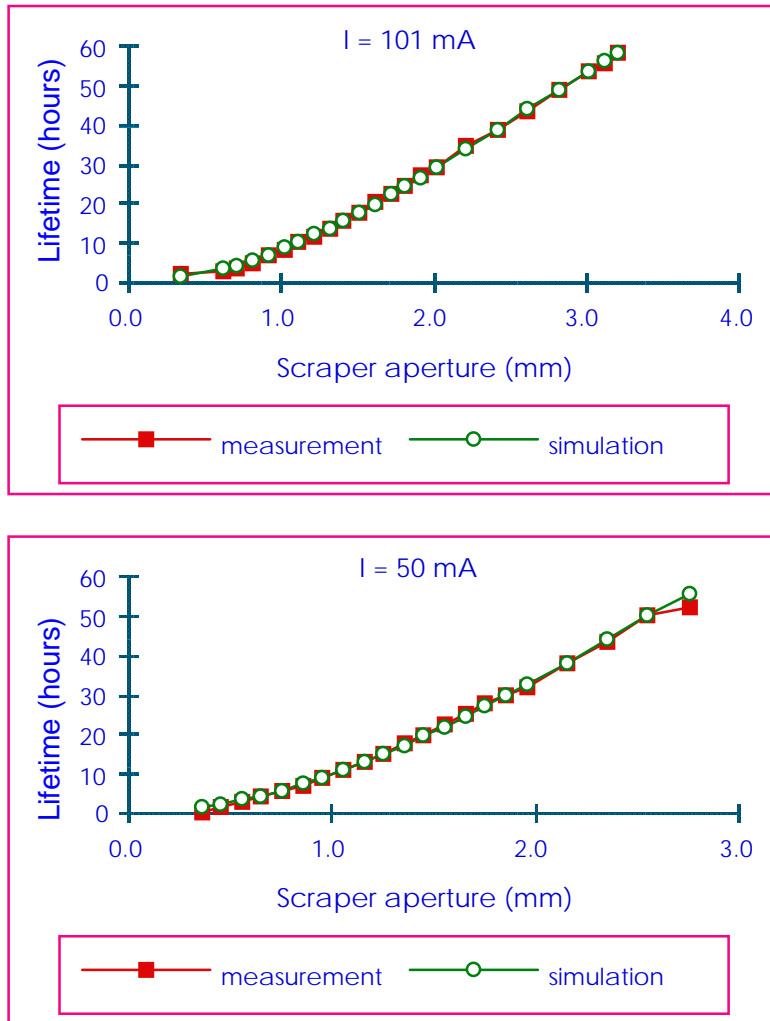


Figure 35: Fit of the lifetime versus scraper measurements

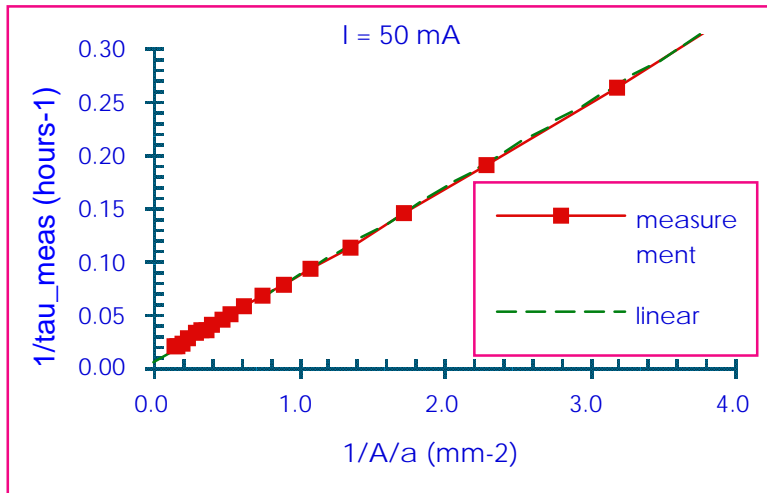
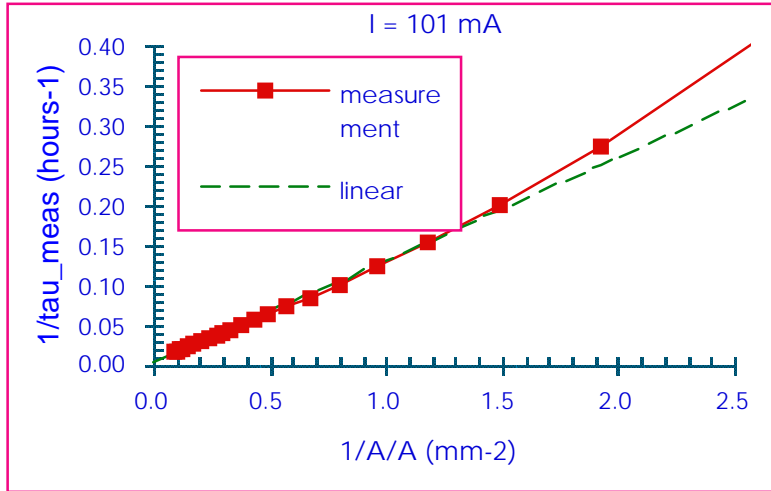


Figure 36: Linear dependence of  $\frac{1}{\tau_{meas}}$  on  $\frac{1}{A^2}$

Table 6

	I = 101 mA	I = 50 mA
average pressure (nT)	0.541	0.46
scraper offset (mm)	29.22	29.16

The resulting pressures are not dramatically different from the ones obtained in the standard  $V_{RF}$  gas scattering experiment. However, even if this does not show up clearly on the graphs, the convergence of the fits is more difficult. This is reflected in the behaviour of the loss rate (see Figure 37), which remains to be understood.

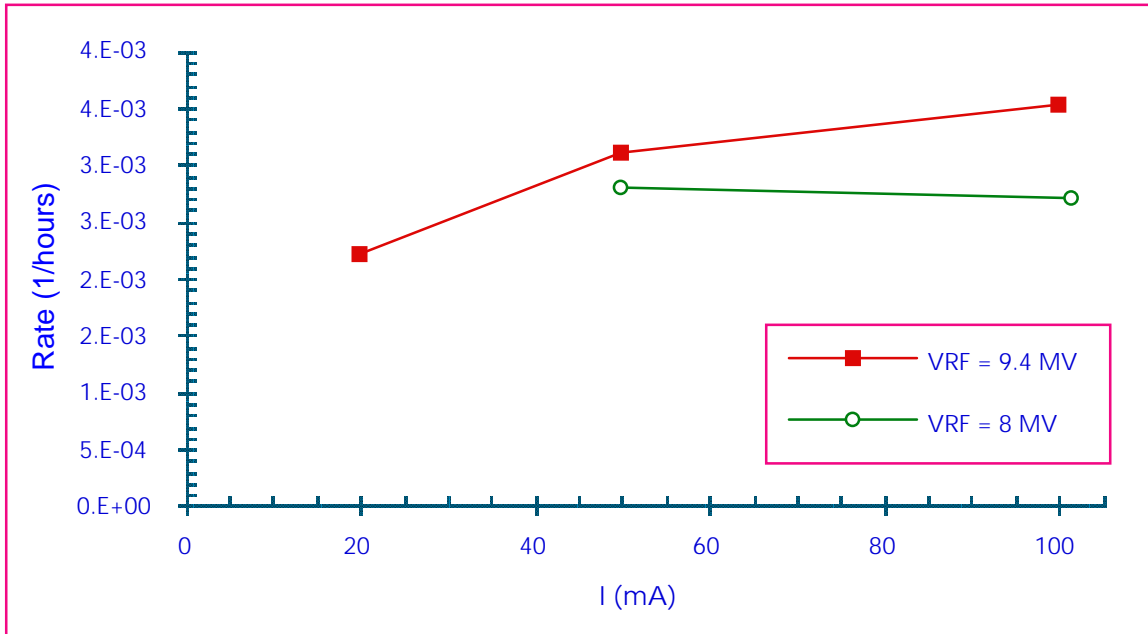


Figure 37: Evolution of the gas rate with the rf voltage

## **Conclusions**

New measuring techniques have been applied for characterizing the lifetime with positrons and for quoting the different contributions.

The linear dependence of the lifetime on the inverse square of the vertical aperture was used to derive the elastic gas scattering rate from the lifetime data when scraping the beam with a vertical scraper. The  $I^{2/3}$  dependence of the Touschek lifetime was used to extract the global gas rate from the lifetime evolution with filling patterns and intensity. The resulting elastic and inelastic gas scattering rates look credible.

The energy acceptance derived from the single bunch lifetime dependence on rf voltage is clearly transversally limited.

The main sources of uncertainties result from the scraper calibration and from the measured transverse emittances and bunch length. This explains the difficulties in modeling very precisely a lifetime that is mainly Touschek dominated.



These measurements offer attractive guidelines for updating the different loss rates after having switched to electrons.

### **Acknowledgements**

Many thanks to M. Borland, L. Emery, and N. Sereno for conducting the machine studies shifts.

Results shown in this report are derived from work performed at Argonne National Laboratory. Argonne is operated by the University of Chicago for the U.S. Department of Energy under Contract No. W-31-109-ENG-38.